

Probing Majorana Neutrino at Future Electron Collider

张亮亮

浙江大学

2016 年 8 月 25 日

In collaboration with M.-x Luo, K. Wang, etc

FRAMEWORK

- Introduction
 - Dirac neutrino → Majorana neutrino
 - The experimental search for Majorana neutrino

- the Inverse $0\nu\beta\beta$ Signal and Collider Phenomenology

- The analysis of signals and backgrounds
 - Collider Phenomenology at ILC/CLIC— $e^- e^-$ collider

- Results and Summary

introduce Majorana neutrinos to the SM

★ Neutrino oscillation → massive neutrino m_ν → Dirac or Majorana type? → unknown

If Dirac neutrino,

- $y_\nu \rightarrow m_\nu$, $\frac{y_\nu}{y_t} \rightarrow$ huge hierarchy → obscure and unnatural
- Such a scenario would be rather uninteresting from an experimental point of view.

Majorana neutrino and charge quantization from anomaly free constraint

A. The SM case:

In the SM, neutrinos keep massless exactly, and triangular anomaly free

$$\begin{aligned} \text{Tr } U(1)_Y [SU(3)_C]^2 &= 0, \quad \text{Tr } U(1)_Y [SU(2)_L]^2 = 0 \\ \text{Tr } [U(1)_Y]^3 &= 0, \quad \text{Tr } [U(1)_Y] (\text{gravitational anomaly}) = 0 \\ \Rightarrow 2Y_q - U_u - Y_d &= 0, \quad 3Y_q + Y_l = 0 \\ 6Y_q^3 - 3Y_u^3 - 3Y_d^3 + 2Y_l^3 - Y_e^3 &= 0 \\ 6Y_q + 2Y_l - 3Y_u - 3Y_d - Y_e &= 0 \end{aligned} \quad (1)$$

$$\Rightarrow Y_q = -\frac{1}{3}Y_l, Y_u = -\frac{4}{3}Y_l, Y_d = \frac{2}{3}Y_l, Y_e = 2Y_l \quad (2)$$

$$\Rightarrow Y_q = -\frac{1}{3}Y_l, Y_u = -\frac{4}{3}Y_l, Y_d = \frac{2}{3}Y_l, Y_e = 2Y_l \quad (3)$$

Only one Higgs doublet in the SM, and we redefine $U(1)$ gauge coupling to make $Y_\phi = +1$.

$$Q = I_{3L} + \frac{Y}{2} \quad (4)$$

The gauge invariance of the Yukawa Lagrangian

$$\mathcal{L}_Y = y_u \bar{Q}_L \tilde{\phi} u_R + y_d \bar{Q}_L \phi d_R + y_e \bar{l} \phi e_R + h.c. \quad (5)$$

$$\Rightarrow Y_u = Y_q + 1, Y_d = Y_q - 1, Y_e = Y_l - 1 \quad (6)$$

\Rightarrow electric charge is quantized in the SM without right-handed neutrino.

Majorana neutrino and charge quantization from anomaly free constraint

B. The SM with Dirac neutrino ν_R , $y_\nu \bar{l}_L \bar{\phi} \nu_R$

$$\begin{aligned} \Rightarrow \quad & 6Y_q^3 - 3Y_u^3 - 3Y_d^3 + 2Y_l^3 - Y_e^3 - Y_\nu^3 = 0 \\ & 6Y_q + 2Y_l - 3Y_u - 3Y_d - Y_e - Y_\nu = 0 \\ & Y_\nu = Y_l + 1 \\ \Rightarrow \quad & Y_\nu \neq 0 (Q_\epsilon \lesssim 10^{-21} e), \text{ Dequantization of electric charge quantization} \end{aligned}$$

C. The SM with Majorana neutrino ν_R

$$\begin{aligned} & \sim \nu_R^T C^{-1} \nu_R \\ \Rightarrow \quad & Y_\nu = 0, \text{ or } Y_l = -1 \rightarrow \text{quantization of electric charge} \end{aligned}$$

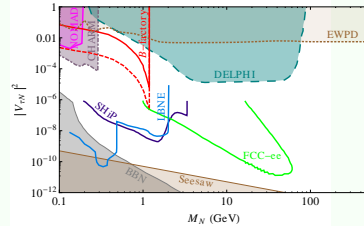
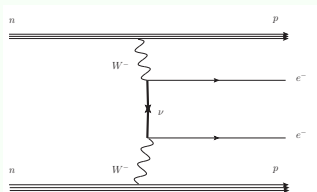
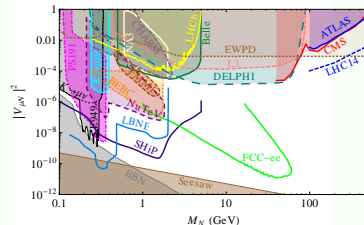
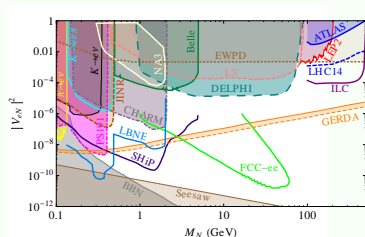
Phys. Rev. D **41**, 271; Phys. Rev. A **7**, 1224; Phys. Rev. D **37**, 3107

* $m_\nu \Rightarrow$ strong hint \rightarrow BSM

\rightarrow *Majorana neutrino*

The simplest and the most economic extension to SM—Seesaw type-I

The experimental search for Majorana neutrino



the presence of Majorana CP phases the occurrence of the cancellation among amplitudes from $0\nu\beta\beta$ would significantly weaken the limits with the number of sterile Majorana neutrinos

New J.Phys.17,no.7,075019 (2015)

the signals for inverse $0\nu\beta\beta$ at $e^- e^-$ collider



Figure: inverse $0\nu\beta\beta$ decay, $e^- e^- \rightarrow W^- W^-$

The different decay modes for the signal of $e^- e^- \rightarrow W^- W^-$

- Pure hadronic decay, $e^- e^- \rightarrow W^- W^- \rightarrow 4j$
- Semileptonic decay, $e^- e^- \rightarrow W^- W^- \rightarrow 2j + \ell^- + \cancel{E}_T$
- Pure leptonic decay, $e^- e^- \rightarrow W^- W^- \rightarrow 2\ell^- + \cancel{E}_T$

the different backgrounds for signals

- Pure hadronic decay, $e^- e^- \rightarrow W^- W^- \rightarrow 4j$

Bkgs: $e^- e^- \rightarrow W^- W^- \nu_e \nu_e$, $e^- e^- \rightarrow W^- Z e^- \nu_e$, $e^- e^- \rightarrow Z Z e^- e^-$,
 $e^- e^- \rightarrow W^- W^+ e^- e^-$, $\gamma\gamma \rightarrow W^+ W^-$

- Semi-leptonic decay, $e^- e^- \rightarrow W^- W^- \rightarrow \ell^- + 2j + \not{E}_T$

*. $e^- e^- \rightarrow W^- W^- \rightarrow e^- + 2j + \not{E}_T$

Bkgs: $e^- e^- \rightarrow W^- W^- \nu_e \nu_e$, $e^- e^- \rightarrow Z W^- e^- \nu_e$, $e^- e^- \rightarrow W^- e^- \nu_e$, $\gamma\gamma \rightarrow W^+ W^-$

*. $e^- e^- \rightarrow W^- W^- \rightarrow \mu^- + 2j + \not{E}_T$

Bkgs: $e^- e^- \rightarrow W^- W^- \nu_e \nu_e$, $\gamma\gamma \rightarrow W^+ W^-$

- Pure leptonic decay, $e^- e^- \rightarrow W^- W^- \rightarrow 2\ell^- + \not{E}_T$

*. $e^- e^- \rightarrow W^- W^- \rightarrow 2e^- + \not{E}_T$

Bkgs: $e^- e^- \rightarrow W^- W^- \nu_e \nu_e$, $e^- e^- \rightarrow Z W^- e^- \nu_e$, $e^- e^- \rightarrow W^- e^- \nu_e$, $e^- e^- \rightarrow Z e^- e^-$

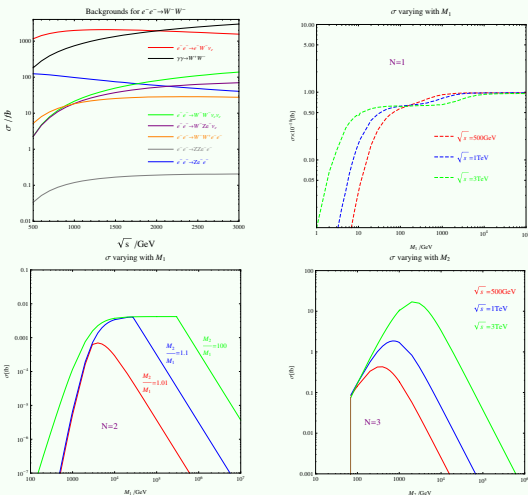
*. $e^- e^- \rightarrow W^- W^- \rightarrow \mu^- e^- + \not{E}_T$

Bkgs: $e^- e^- \rightarrow W^- W^- \nu_e \nu_e$, $e^- e^- \rightarrow Z W^- e^- \nu_e$, $e^- e^- \rightarrow W^- e^- \nu_e$

*. $e^- e^- \rightarrow W^- W^- \rightarrow 2\mu^- + \not{E}_T$

Bkgs: $e^- e^- \rightarrow W^- W^- \nu_e \nu_e$

The cross sections of different backgrounds and signals production



Phys. Rev. D **92**, no. 9, 094012 (2015)



In order to clearly present the boosted effect of W boson , we only analyse the collider phenomenology for inverse $0\nu\beta\beta$ with $\sqrt{s} = 500$ GeV and 3 TeV

For $\sqrt{s} = 500$ GeV, the basic cuts is given by

$$\begin{aligned} P_{T\ell} &> 10 \text{ GeV}, P_{Tj} > 20 \text{ GeV}, |\eta_\ell| < 2.5 \\ \Delta R_{jj} &> 0.4, \Delta R_{\ell\ell} > 0.4, \Delta R_{\ell j} > 0.4, |\eta_j| < 5 \end{aligned} \quad (7)$$

For $\sqrt{s} = 3$ TeV, the basic cuts is given by

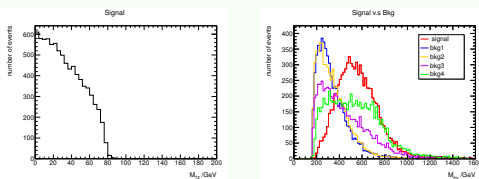
$$\begin{aligned} P_{T\ell} &> 10 \text{ GeV}, P_{Tj} > 20 \text{ GeV}, |\eta_\ell| < 2.5 \\ \Delta R_{\ell\ell} &> 0.4, \Delta R_{\ell j} > 0.4, |\eta_j| < 5 \end{aligned} \quad (8)$$

Pure leptonic decay with $\sqrt{s} = 500$ GeV

$$m_X^2 \geq M_{T2}^2 \equiv \min_{\not{p}_1 + \not{p}_2 = \not{p}_T} [\max\{m_T^2(\not{p}_{T\ell}, \not{p}_1), m_T^2(\not{p}_{T\ell}, \not{p}_2)\}]$$

Phys. Lett. B **463** (1999) 99

*. $e^- e^- \rightarrow W^- W^- \rightarrow 2e^- + \not{E}_T$



The distributions of M_{T2} , $M_{f.s.}$ and $\cos \theta_{\mu e}$, bkg1(blue): $e^- e^- \rightarrow W^- W^- 2\nu_e$, bkg2(orange): $e^- e^- \rightarrow ZW^- e^- \nu_e$, bkg3(violet): $e^- e^- \rightarrow W^- e^- \nu_e$, bkg4(green): $e^- e^- \rightarrow Z2e^-$

Table: Signal v.s Bkg

Process	Basic Cuts($\sigma \sim fb$)	$2e^-$ required(ϵ)	$M_{f.s.} > 400$ GeV(ϵ)	$M_{f.s.} > 450$ GeV(ϵ)
Signal	5.0×10^{-3}	0.84	0.68	0.6
Bkg1	2.57×10^{-2}	0.83	0.15	0.1
Bkg2	4.7×10^{-2}	0.84	0.17	0.11
Bkg3	120.8	0.83	0.3	0.25
Bkg4	24.7	0.84	0.5	0.44

Pure leptonic decay with $\sqrt{s} = 500 \text{ GeV}$

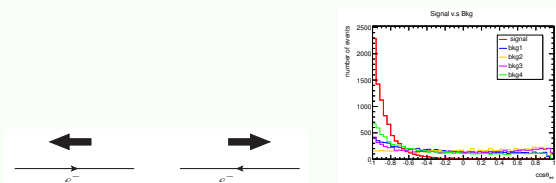


Figure: The distribution of $\cos \theta_{ee}$, bkg1(blue): $e^- e^- \rightarrow W^- W^- 2\nu_e$, bkg2(orange): $e^- e^- \rightarrow ZW^- e^- \nu_e$, bkg3(purple): $e^- e^- \rightarrow W^- e^- \nu_e$, bkg4(green): $e^- e^- \rightarrow Z2e^-$

Table: Signal v.s Bkg

Process	Basic Cuts($\sigma \sim fb$)	$2e^- (\epsilon)$	$\cos \theta_{ee} < -0.7(\epsilon)$	$\cos \theta_{ee} < -0.8$	$\cos \theta_{ee} < -0.9(\epsilon)$
Signal	5.0×10^{-3}	0.84	0.73	0.63	0.43
Bkg1	2.57×10^{-2}	0.83	0.23	0.17	0.09
Bkg2	4.7×10^{-2}	0.84	0.12	0.08	0.04
Bkg3	120.8	0.83	0.19	0.15	0.09
Bkg4	24.7	0.84	0.31	0.25	0.15

Pure leptonic decay with $\sqrt{s} = 3$ TeV

The distributions of $M_{f.s.}$ and $\cos \theta_{ee}$:

we assume that $c_1=c_2=c$, then $\sqrt{(c\vec{p}_{1T\ell} + c\vec{p}_{2T\ell})^2} = E_T$, $(p_{\nu_\ell} + p_\ell)^2 = m_W^2$.

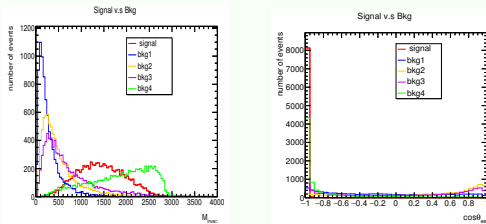


Figure: bkg1(blue): $e^- e^- \rightarrow W^- W^- 2\nu_e$, bkg2(orange): $e^- e^- \rightarrow ZW^- e^- \nu_e$, bkg3(violet): $e^- e^- \rightarrow W^- e^- \nu_e$, bkg4(green): $e^- e^- \rightarrow Ze^- e^-$

Pure leptonic decay with $\sqrt{s} = 3$ TeV

Table: Signal v.s Bkg

Process	Basic Cuts($\sigma \sim fb$)	$2e^-$ required(ϵ)	$900 \text{ GeV} < M_{\text{inv.}} < 1900 \text{ GeV}(\epsilon)$
Signal	0.18	0.82	0.52
Bkg1	1.3	0.83	0.03
Bkg2	1.15	0.83	0.1
Bkg3	124.5	0.83	0.18
Bkg4	8	0.82	0.29

Table: Signal v.s Bkg

Process	Basic Cuts($\sigma \sim fb$)	$2e^-$ required(ϵ)	$\cos \theta_{ee} < -0.96(\epsilon)$	$\cos \theta_{ee} < -0.99(\epsilon)$
Signal	0.18	0.82	0.81	0.71
Bkg1	1.3	0.83	0.04	0.01
Bkg2	1.15	0.83	0.02	0.006
Bkg3	124.5	0.83	0.07	0.03
Bkg4	8	0.82	0.41	0.24

Pure leptonic decay with $\sqrt{s} = 500$ GeV

*. $e^- e^- \rightarrow W^- W^- \rightarrow \mu^- e^- + \not{E}_T$

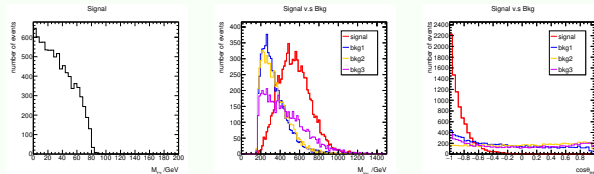


Figure: The distributions of M_{T2} , $M_{f.s.}$ and $\cos \theta_{\mu e}$. bkg1(blue): $e^- e^- \rightarrow W^- W^- 2\nu_e$, bkg2(orange): $e^- e^- \rightarrow W^- Ze^- \nu_e$, bkg3(violet): $e^- e^- \rightarrow W^- e^- \nu_e$

Table: Signal v.s Bkg

Process	Basic Cuts($\sigma \sim fb$)	$\mu^- + e^- (\epsilon)$	$M_{f.s.} > 400\text{GeV}(\epsilon)$
Signal	1.0×10^{-2}	0.87	0.70
Bkg1	5.14×10^{-2}	0.85	0.16
Bkg2	4.7×10^{-2}	0.85	0.17
Bkg3	120.8	0.80	0.29

Process	Basic Cuts($\sigma \sim fb$)	$\mu^- + e^- (\epsilon)$	$\cos \theta_{\mu e} < -0.7(\epsilon)$
Signal	1.0×10^{-2}	0.87	0.75
Bkg1	5.14×10^{-2}	0.85	0.24
Bkg2	4.7×10^{-2}	0.85	0.12
Bkg3	120.8	0.80	0.19

Pure leptonic decay with $\sqrt{s} = 3$ TeV

The distributions of $M_{f.s.}$ and $\cos \theta_{\mu e}$

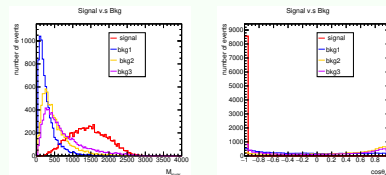


Figure: bkg1(blue): $e^- e^- \rightarrow W^- W^- 2\nu_e$, bkg2(orange): $e^- e^- \rightarrow W^- Z e^- \nu_e$, bkg3(violet): $e^- e^- \rightarrow W^- e^- \nu_e$

Table: Signal v.s Bkg

Process	Basic Cuts($\sigma \sim fb$)	$\mu^- + e^- (\epsilon)$	$M_{f.s.} > 900\text{GeV} (\epsilon)$
Signal	0.37	0.86	0.72
Bkg1	2.6	0.83	0.03
Bkg2	1.15	0.82	0.11
Bkg3	124.5	0.83	0.23
Process	Basic Cuts($\sigma \sim fb$)	$\mu^- + e^- (\epsilon)$	$\cos \theta_{\mu e} < -0.95 (\epsilon)$
Signal	0.37	0.86	0.86
Bkg1	2.6	0.83	0.05
Bkg2	1.15	0.82	0.02
Bkg3	124.5	0.83	0.08

Pure leptonic decay with $\sqrt{s} = 500 \text{ GeV}$

*. $e^- e^- \rightarrow W^- W^- \rightarrow 2\mu^- + \cancel{E}_T$

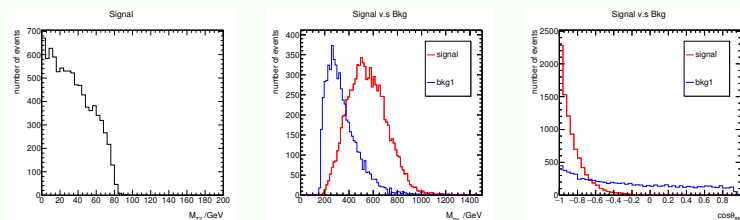


Figure: The distributions of M_{T2} , $M_{f.s.}$ and $\cos \theta_{\mu\mu}$. bkg1(blue): $e^- e^- \rightarrow W^- W^- 2\nu_e$

Table: Signal v.s Bkg

Process	Basic Cuts($\sigma \sim fb$)	$2\mu^- (\epsilon)$	$M_{f.s.} > 400 \text{ GeV} (\epsilon)$
Signal	5.0×10^{-3}	0.90	0.73
Bkg1	2.57×10^{-2}	0.87	0.16
Process	Basic Cuts($\sigma \sim fb$)	$2\mu^- (\epsilon)$	$\cos \theta_{\mu\mu} < -0.7 (\epsilon)$
Signal	5.0×10^{-3}	0.90	0.78
Bkg1	2.57×10^{-2}	0.87	0.24

Pure leptonic decay with $\sqrt{s} = 3$ TeV

The distributions of $M_{f.s.}$ and $\cos \theta_{\mu\mu}$

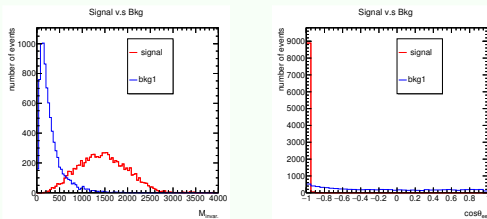


Figure: bkg1(blue): $e^- e^- \rightarrow W^- W^- 2\nu_e$

Table: Signal v.s Bkg

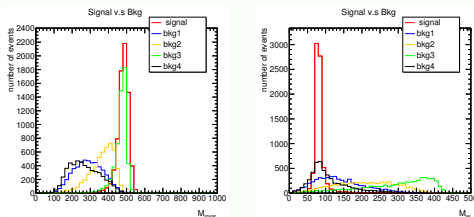
Process	Basic Cuts($\sigma \sim fb$)	$2\mu^-$ required(ϵ)	$M_{inv.} > 700$ GeV(ϵ)
Signal	0.18	0.90	0.83
Bkg1	1.3	0.82	0.06
Process	Basic Cuts($\sigma \sim fb$)	$2\mu^-$ required(ϵ)	$\cos \theta_{\mu\mu} < -0.95$ (ϵ)
Signal	0.18	0.90	0.89
Bkg1	1.3	0.82	0.05

Semileptonic decay with $\sqrt{s} = 500$ GeV

*. $e^- e^- \rightarrow W^- W^- \rightarrow e^- + 2j + \not{E}_T$

the distributions of $M_{f.s.}$ and M_W

$$\vec{p}_{T\nu\ell} = - \sum_i \vec{p}_{Ti}(\text{observed}) \quad p_{z\nu\ell} = - \sum_i p_{zi}(\text{observed}) \quad (9)$$



bkg1(blue): $e^- e^- \rightarrow W^- W^- 2\nu_e$, bkg2(orange): $e^- e^- \rightarrow ZW^- e^- \nu_e$, bkg3(green): $e^- e^- \rightarrow W^- e^- \nu_e$,
bkg4(black): $\gamma\gamma \rightarrow W^+ W^-$

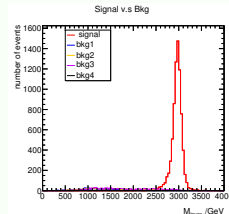
Table: Signal v.s Bkg

Process	Basic Cuts($\sigma \sim fb$)	$2j + e^- (\epsilon)$	$400\text{GeV} < M_{f.s.} < 550\text{GeV}$	$70\text{GeV} < M_W < 90\text{GeV} (\epsilon)$
Signal	5.64×10^{-2}	0.73	0.71	0.57
Bkg1	0.23	0.52	0.046	0.003
Bkg2	0.2	0.52	0.18	0.002
Bkg3	537.3	0.54	0.51	0.007
Bkg4	8	0.51	0.037	0.006

Semileptonic decay with $\sqrt{s} = 3$ TeV

The distributions of $M_{2j\ell\nu}$ for signal and backgrounds

$$\vec{p}_{\nu\ell} \simeq c\vec{p}_\ell, c \text{ is a constant i.e. } p_T(\nu_e) = \not{E}_T, p_z(\nu_e) = p_z(e) \times \frac{\not{E}_T}{p_T(e)}$$



bkg1(blue): $e^- e^- \rightarrow W^- W^- 2\nu_e$, bkg2(orange): $e^- e^- \rightarrow ZW^- e^- \nu_e$, bkg3(violet): $e^- e^- \rightarrow W^- e^- \nu_e$, bkg4(black): $\gamma\gamma \rightarrow W^+ W^-$

Table: Signal v.s Bkg

Process	Basic Cuts($\sigma \sim fb$)	$1j_W + e^- (\epsilon)$	$M_{f,s} > 2.5\text{TeV}(\epsilon)$	$M_{f,s} > 2.7\text{TeV}(\epsilon)$	$M_{f,s} > 2.8\text{TeV}(\epsilon)$
Signal	2.2	0.77	0.76	0.74	0.71
Bkg1	13.2	0.06	0.004	0.0027	0.0023
Bkg2	6.8	0.074	0.01	0.0069	0.0052
Bkg3	774.5	0.092	0.02	0.014	0.011
Bkg4	113	0.006	0.0003	0.0003	0.0002

Semileptonic decay with $\sqrt{s} = 500$ GeV

*. $e^- e^- \rightarrow W^- W^- \rightarrow \mu^- + 2j + \cancel{E}_T$

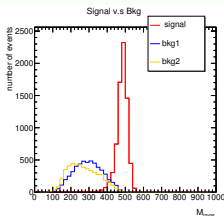


Figure: bkg1(blue): $e^- e^- \rightarrow W^- W^- 2\nu_e$, bkg2(orange): $\gamma\gamma \rightarrow W^+ W^-$

Table: Signal v.s Bkg

Process	Basic Cuts($\sigma \sim fb$)	$2j + \mu^- (\epsilon)$	$M_{f.s.} > 400\text{GeV} (\epsilon)$
Signal	5.64×10^{-2}	0.74	0.72
Bkg1	0.23	0.52	0.05
Bkg2	8	0.49	0.04

Semileptonic decay with $\sqrt{s} = 3$ TeV

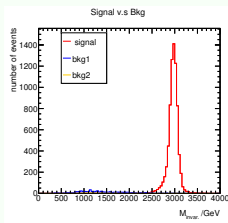


Figure: bkg1(blue): $e^- e^- \rightarrow W^- W^- 2\nu_e$, bkg2(orange): $\gamma\gamma \rightarrow W^+ W^-$

Table: Signal v.s Bkg

Process	Basic Cuts($\sigma \sim fb$)	$1j_W + \mu^- (\epsilon)$	$M_{f.s} > 2.5\text{TeV}(\epsilon)$
Signal	2.2	0.75	0.75
Bkg1	13.2	0.06	0.0026
Bkg2	113	0.005	0.0002

Hadronic decay with $\sqrt{s} = 500$ GeV

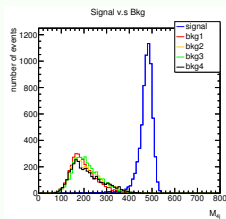


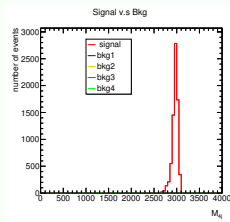
Figure: The distributions of M_{4j} , bkg1(red): $e^- e^- \rightarrow W^- W^- \nu_e \nu_e$,
bkg2(orange): $e^- e^- \rightarrow W^- W^+ e^- e^-$, bkg3(green): $e^- e^- \rightarrow W^- Z e^- \nu_e$, bkg4(black):
 $\gamma\gamma \rightarrow W^+ W^-$

Table: Signal v.s Bkg

Process	Basic Cuts($\sigma \sim fb$)	$4j$ required(ϵ)	$M_{4j} > 350\text{GeV}(\epsilon)$	$M_{4j} > 400\text{GeV}(\epsilon)$
Signal	0.16	0.66	0.65	0.63
Bkg1	0.5	0.35	0.0053	0.0006
Bkg2	1	0.36	0.013	0.0027
Bkg3	0.4	0.37	0.0095	0.0022
Bkg4	34.4	0.33	0.016	0.0031

Hadronic decay with $\sqrt{s} = 3$ TeV

M_{2j_W} distributions for backgrounds



Bkg1(red): $e^- e^- \rightarrow W^- W^- 2\nu_e$, Bkg2(orange): $e^- e^- \rightarrow W^+ W^- e^- e^-$, Bkg3(violet): $e^- e^- \rightarrow ZW^- e\nu_e$,
Bkg4(green): $\gamma\gamma \rightarrow W^+ W^-$

Table: Signal v.s Bkg

Process	Basic Cuts($\sigma \sim fb$)	$2j_W, \Delta R_{jj} > 0.4(\epsilon)$	$M_{2j} > 2000\text{GeV}(\epsilon)$	$M_{2j} > 2300\text{GeV}(\epsilon)$
Signal	6.7	0.73	0.73	0.73
Bkg1	34.4	0.011	0.0009	0.0001
Bkg2	6	0.018	0.0026	0.001
Bkg3	12	0.007	0.0011	0.0004
Bkg4	600	0.0033	0.0002	0

Results and Summary

$\sqrt{s} = 500 \text{ GeV}, \mathcal{L} = 500 \text{ fb}^{-1}$; $\sqrt{s} = 3 \text{ TeV}, \mathcal{L} = 3000 \text{ fb}^{-1}$

- $e^- e^- \rightarrow W^- W^- \rightarrow 2\mu^- + \cancel{E}_T$

For $\sqrt{s} = 500 \text{ GeV}$, $\frac{S}{S+B} \simeq 40\%$, $\frac{S}{\sqrt{S+B}} \simeq 1$; For $\sqrt{s} = 3 \text{ TeV}$, $\frac{S}{S+B} \simeq 70\%$, $\frac{S}{\sqrt{S+B}} \simeq 18$

- $e^- e^- \rightarrow W^- W^- \rightarrow e^- + 2j + \cancel{E}_T$

For $\sqrt{s} = 3 \text{ TeV}$, $\frac{S}{S+B} \simeq 16\%$, $\frac{S}{\sqrt{S+B}} \simeq 26$

- $e^- e^- \rightarrow W^- W^- \rightarrow \mu^- + 2j + \cancel{E}_T$

For $\sqrt{s} = 500 \text{ GeV}$, $\frac{S}{S+B} \simeq 11\%$, $\frac{S}{\sqrt{S+B}} \simeq 1.5$; For $\sqrt{s} = 3 \text{ TeV}$, $\frac{S}{S+B} \simeq 96\%$, $\frac{S}{\sqrt{S+B}} \simeq 70$

- $e^- e^- \rightarrow W^- W^- \rightarrow 4j$

For $\sqrt{s} = 500 \text{ GeV}$, $\frac{S}{S+B} \simeq 47\%$, $\frac{S}{\sqrt{S+B}} \simeq 4.9$; For $\sqrt{s} = 3 \text{ TeV}$, $\frac{S}{S+B} \simeq 1$, $\frac{S}{\sqrt{S+B}} \simeq 121$

Results and Summary

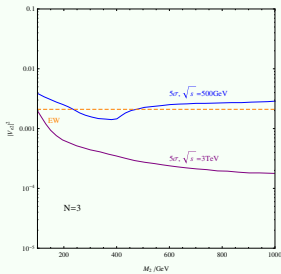
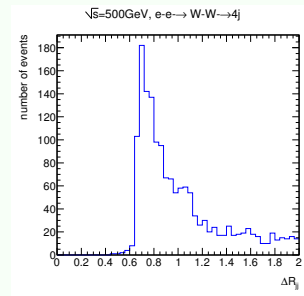


Figure: 5σ discovery limit for $|V_{e2}|^2$ and M_2 with $4j$ final states for $N = 3$, the red dashed line stands for the EWPT bound; the purple line stands for 5σ discovery limit with $\sqrt{s} = 3$ TeV; the blue line stands for 5σ discovery limit with $\sqrt{s} = 500$ GeV

Results and Summary

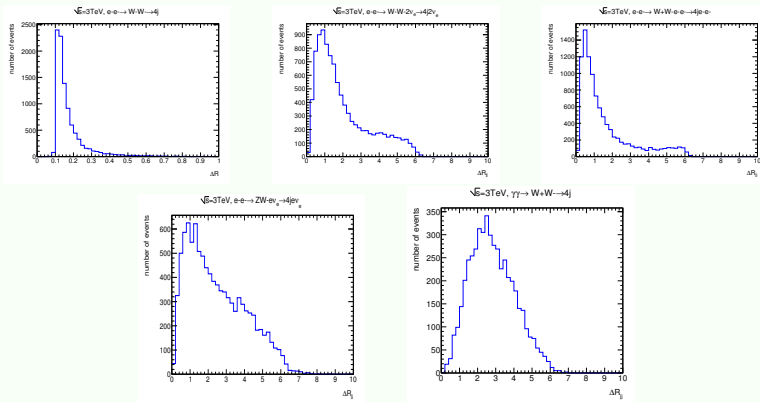
- the necessity to introduce Majorana neutrinos to SM
- we give the detailed analysis of collider phenomenology, and find that for $\sqrt{s} = 3$ TeV the signal will be probed more easily.
- Finally, taking the interference effects into consideration, we give the 5σ discovery limit with $\sqrt{s} = 500$ GeV and 3 TeV for $N = 3$.

Backup

Hadronic decay with $\sqrt{s} = 500$ GeVFigure: The distributions of ΔR_{ij}

Hadronic decay with $\sqrt{s} = 3$ TeV

The distributions of ΔR of jj from W decay for signal and backgrounds



$\Delta R < 0.4 \Rightarrow$ the signal mostly highly boosted $\Rightarrow 2j \rightarrow j_W$